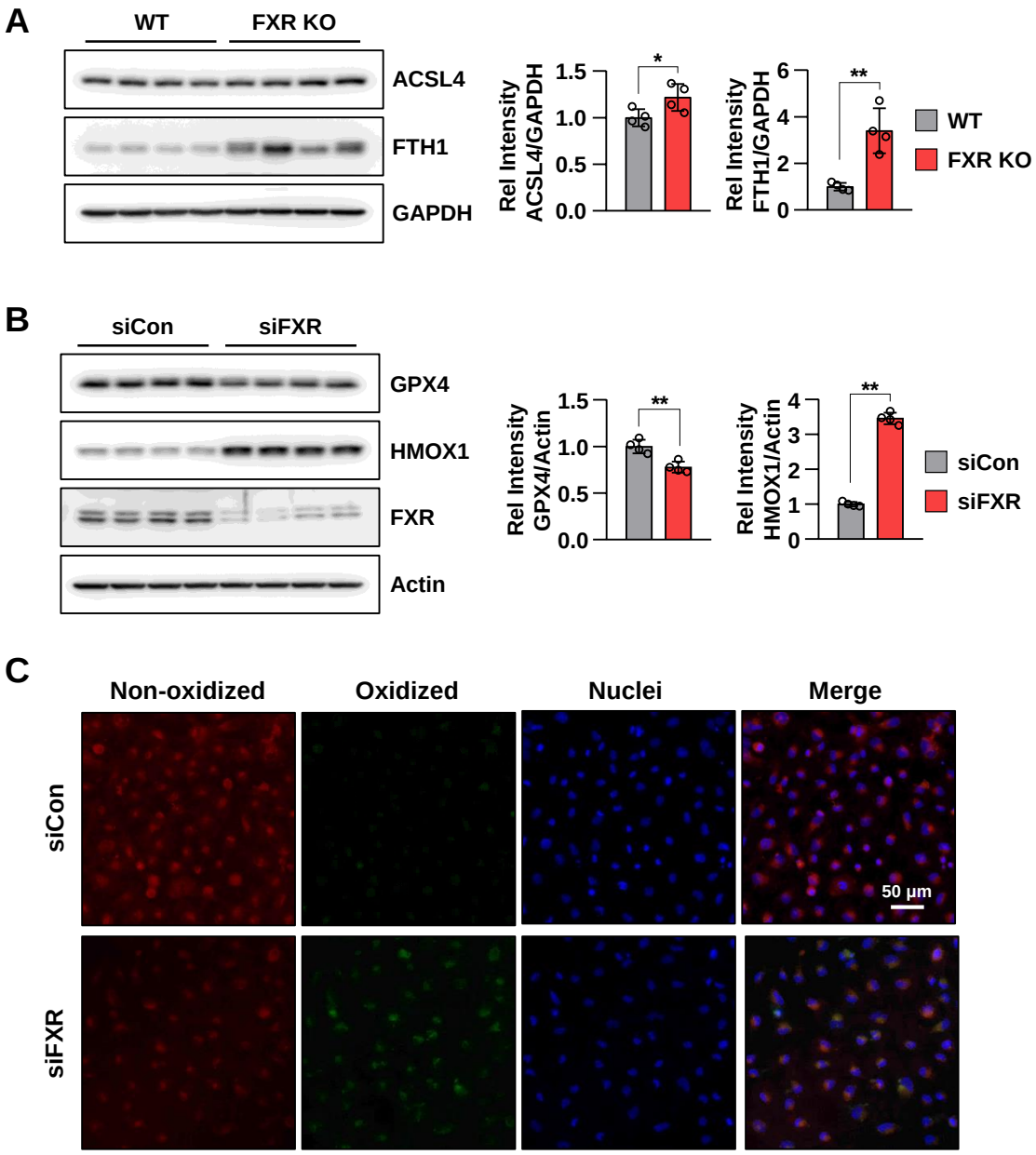

Supplementary Figure 1. FXR deficiency increases ferroptotic responses in mice and HK2 cells. (A) Kidney tissues were collected from wild-type (WT) and FXR knockout (FXR KO) mice. Protein levels of ACSL4 and FTH1 were detected by immunoblotting. The relative protein levels are shown. The values for the WT group were set to 1 (n = 4). (B) HK2 cells were transfected with siControl or siFXR as indicated, and protein levels of GPX4, HMOX1, and FXR were detected by immunoblotting. The relative protein levels are shown. The values for the siControl group were set to 1 (n = 4). (C) HK2 cells were transfected with siControl or siFXR as indicated; 48 h later, the the cells were incubated with C11-BODIPY 581/591 (2 μM) and Hoechst 33258 for counterstaining; the images were then immediately visualized by confocal microscopy. Confocal microscopy showed non-oxidized lipid (red, Texas Red) and oxidized lipid (green, FITC). Scale bar, 50 μm. All values are presented as the mean ± SD. Statistical significance was measured using one-way ANOVA with Bonferroni post hoc-test. *P<0.05, **P<0.005.

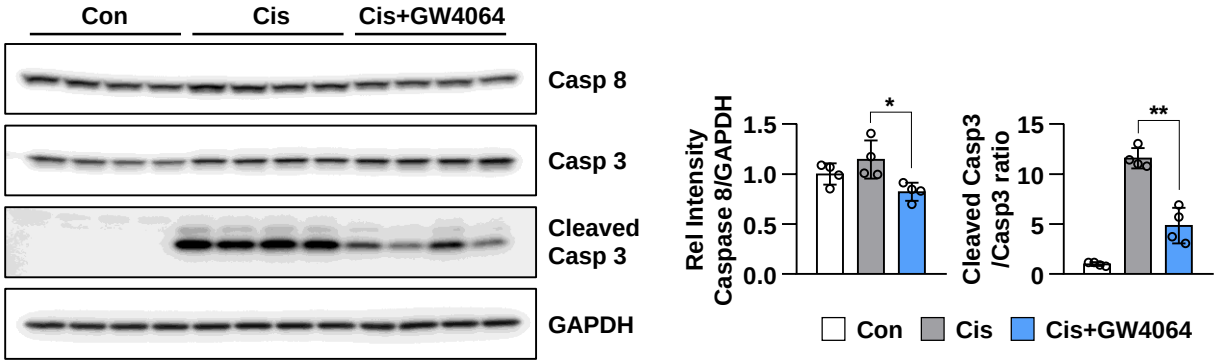

Supplementary Figure 2. GW4064 treatment attenuates apoptosis in cisplatin-induced AKI mice.). The mice were injected with cisplatin (20 mg/kg) on the third day of GW4064 administration. After 48 h of cisplatin injection, the kidneys tissues were collected. Protein levels of caspases 8, caspase 3, and cleaved caspase 3 were detected by immunoblotting. The relative protein levels are shown. The values for the control group were set to 1 (n = 4). All values are presented as the mean ± SD. Statistical significance was measured using one-way ANOVA with Bonferroni post hoc-test. *P<0.05, **P<0.005.

A

GW4064 vs. Veh

KEGG (UP)	*p*-Value
Metabolic pathways	9.66E-13
Glycerolipid metabolism	5.29E-04
Glycine, serine and threonine metabolism	4.66E-03
Glutathione metabolism	1.35E-02
Bile secretion	2.54E-02

KEGG (DOWN)	*p*-Value
Adipocytokine signaling pathway	1.03E-04
Cytokine-cytokine receptor interaction	5.61E-03
Bile secretion	6.99E-03
AMPK signaling pathway	1.08E-02
cAMP signaling pathway	2.99E-02

B

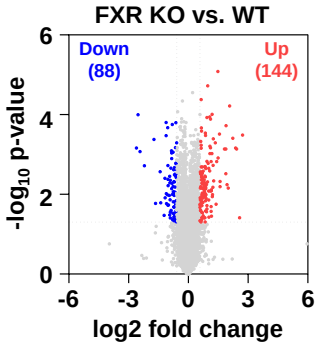

C **FXR KO vs. WT**

GO Term (UP)	*p*_Value
Monocarboxylic acid metabolic process	1.40E-11
Organic acid metabolic process	5.01E-11
Fatty acid metabolic process	6.52E-11
Lipid metabolic process	2.22E-10
Monooxygenase activity	2.06E-06
Iron ion binding	9.70E-06

GO Term (DOWN)	*p*_Value
Extracellular matrix structural constituent	5.01E-18
Collagen-containing extracellular matrix	1.93E-15
Response to oxygen-containing compound	1.09E-05
Cell adhesion	4.29E-05
Response to hormone	3.67E-04

D **FXR KO vs. WT**

KEGG (UP)	*p*-Value
PPAR signaling pathway	2.83E-16
Metabolic pathways	1.00E-13
Fatty acid degradation	5.88E-10
Peroxisome	9.07E-06
p53 signaling pathway	1.60E-03
Cholesterol metabolism	1.08E-02

KEGG (DOWN)	*p*-Value
Protein digestion and absorption	4.20E-15
ECM-receptor interaction	3.31E-12
Focal adhesion	5.42E-11
PI3K-Akt signaling pathway	3.67E-10
Metabolic pathways	3.94E-03

E

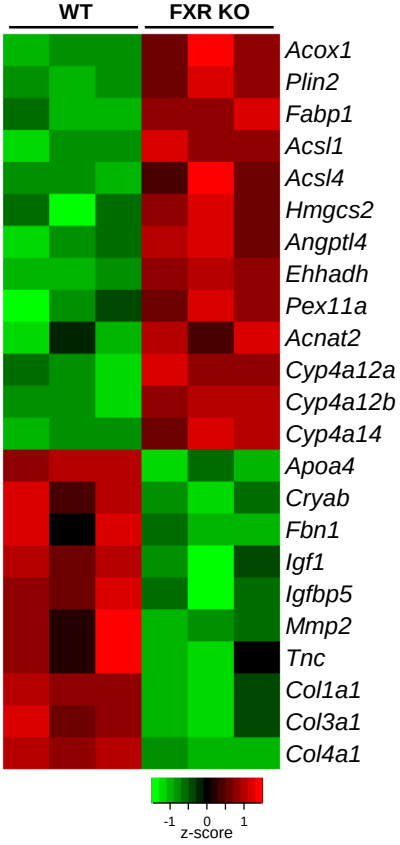

F

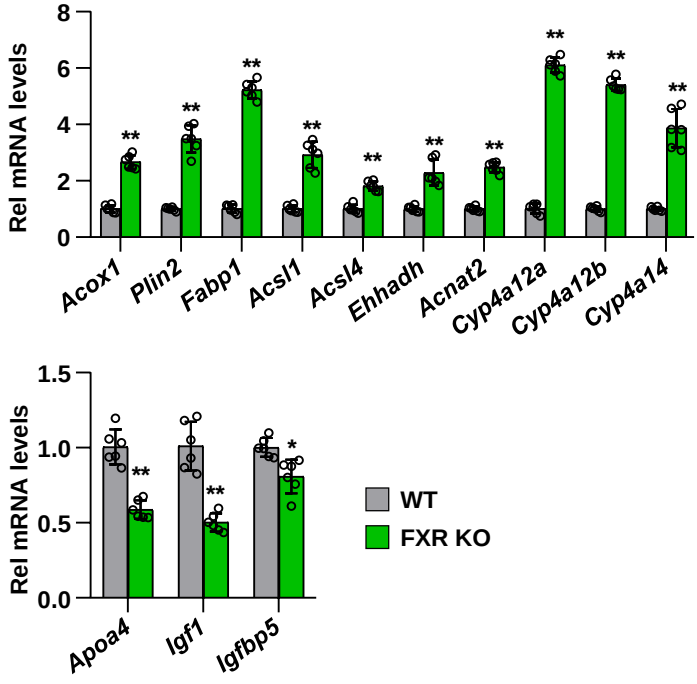

Continue

Supplementary Figure 3. FXR KO mice kidney upregulates the expression of fatty acid metabolic process and peroxisome genes. RNA-Sequencing analysis: (A) Kyoto Encyclopedia of Genes and Genomes (KEGG) analysis of genes either up- or down-regulated in GW4064 treatment vs. Vehicle treatment. (B-F) Vehicle-treated FXR KO mice vs. vehicle-treated WT mice (B) Volcano plots of RNA-Seq data. Blue, down-regulated genes; red, up-regulated genes. (C) Gene ontology (GO) analysis of genes either up- or down-regulated. (D) KEGG analysis of genes either up- or down-regulated. (E) Heat maps showing changes in gene expression in FXR KO mice treated with vehicle compared to WT mice treated with vehicle. (F) The mRNA levels of the selected genes were measured by qRT-PCR (n = 6). The values for vehicle-treated group are set to 1. All values are presented as the mean ± SD. Statistical significance was measured using one-way ANOVA with Bonferroni post hoc-test. *P<0.05, **P<0.005.

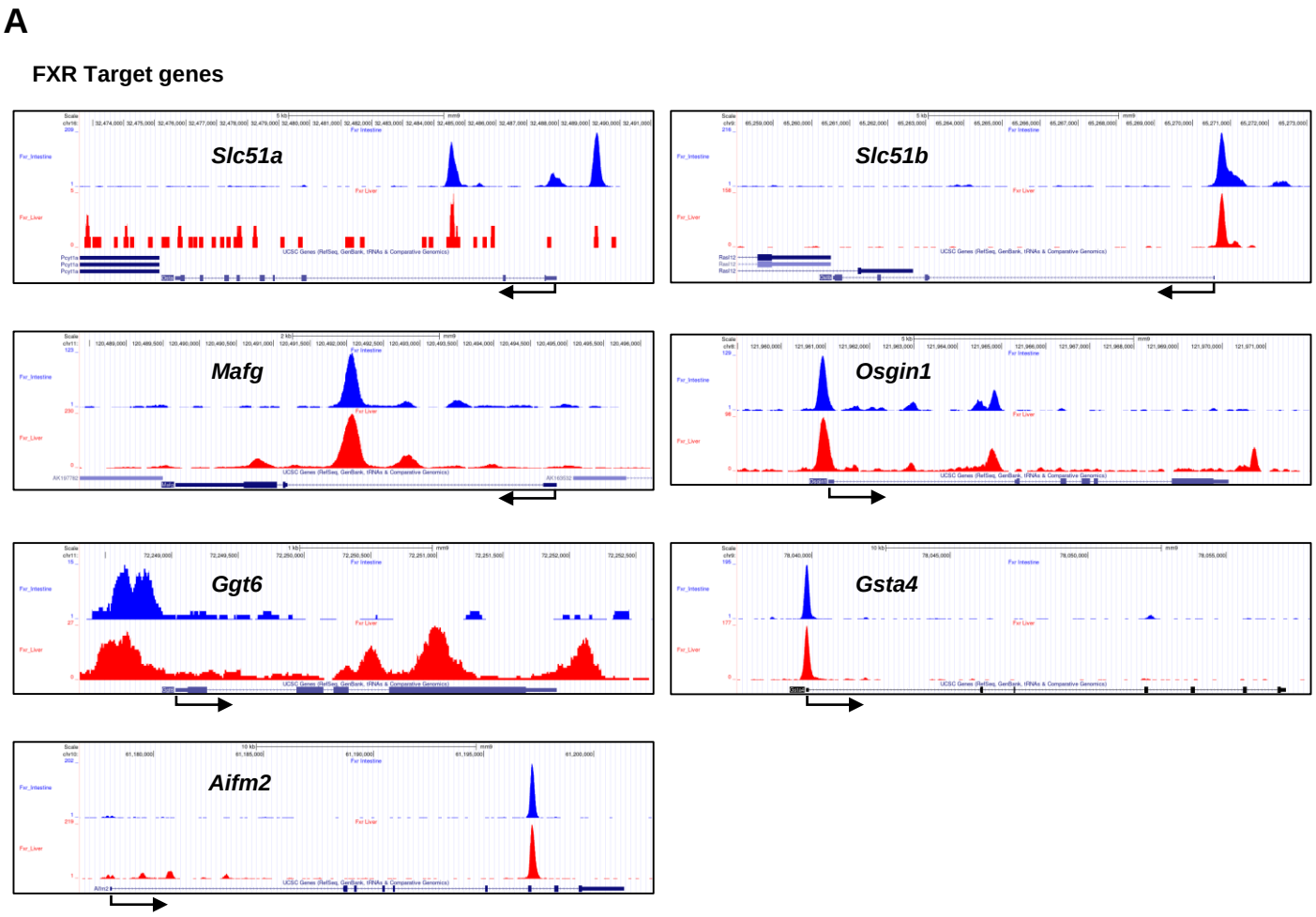

Supplementary Figure 4. Pharmacological activation of FXR increases its binding to ferroptosis associated genes. (A) FXR binding peaks at selected FXR target and ferroptosis genes. Figures were generated from mouse liver and intestine ChIP-seq data using the University of California, Santa Cruz (UCSC) genome browser. The direction of gene transcription is indicated by the arrow and the beginning of the arrow indicates the transcription start site. (B) WT and FXR KO mice were fasted for 16 h, and then, were administrated with the GW4064 or vehicle by oral gavage. At 6 h after administration with GW4064, the kidneys were collected. The mRNA levels of *Aifm2* were measured by qRT-PCR (n = 6). The values for vehicle-treated WT mice group are set to 1. (C) The mice were injected with cisplatin (20 mg/kg) on the third day of administration with GW4064. At 48 h after cisplatin injection, the kidneys were collected. The mRNA levels of *Aifm2* were measured by qRT-PCR (n = 6). The values for control mice group are set to 1. All values are presented as the mean ± SD. Statistical significance was measured using one-way ANOVA with Bonferroni post hoc-test. *P<0.05, **P<0.005, N.S: Not Significant.

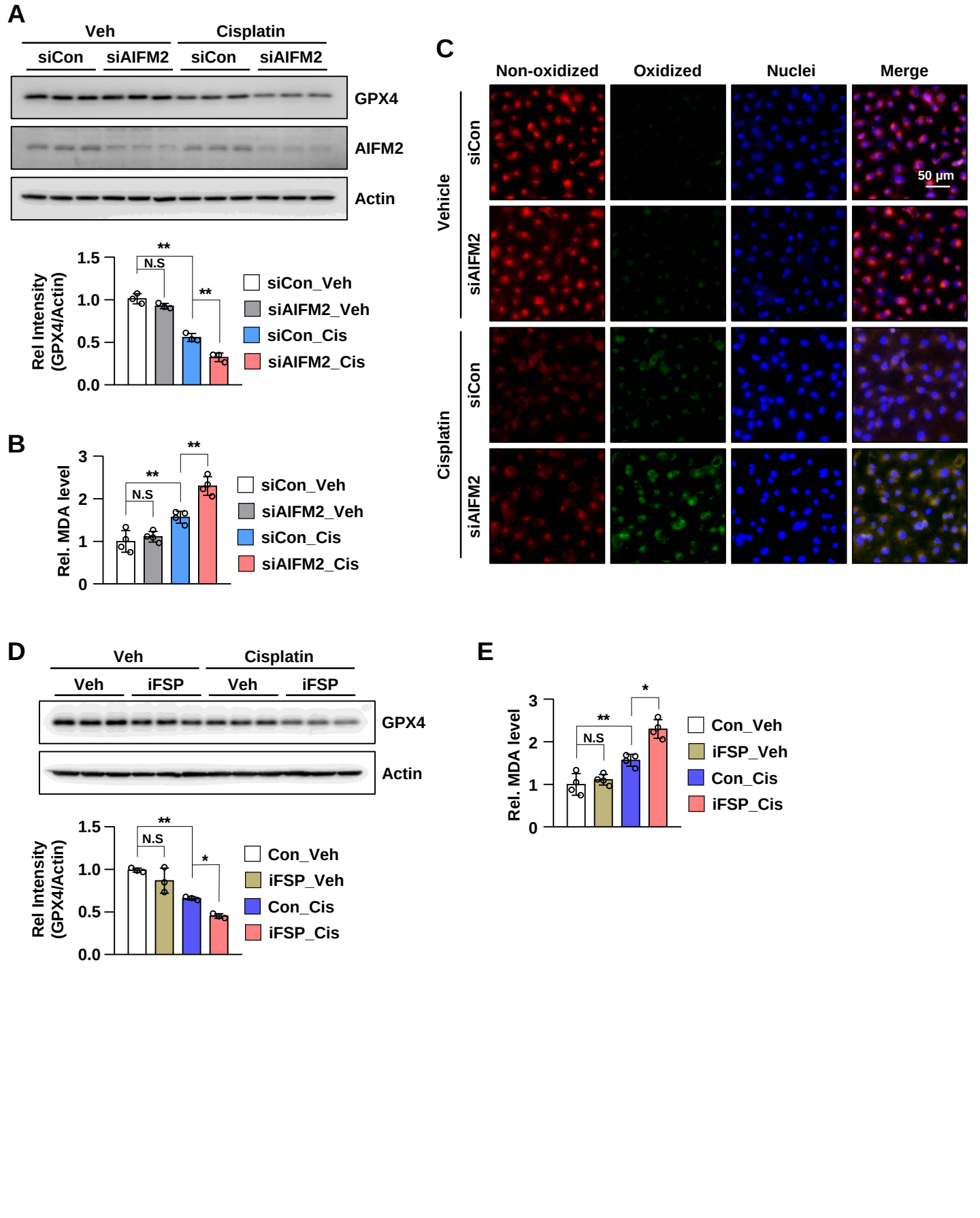
A
Veh
Cisplatin
siCon
siAIFM2
siCon
siAIFM2
GPX4
AIFM2
Actin
Rel Intensity (GPX4/Actin)
1.5
1.0
0.5
0.0
**
N.S
**
siCon_Veh
siAIFM2_Veh
siCon_Cis
siAIFM2_Cis
B
Rel. MDA level
3
2
1
0
**
N.S
**
siCon_Veh
siAIFM2_Veh
siCon_Cis
siAIFM2_Cis
C
Non-oxidized
Oxidized
Nuclei
Merge
Vehicle
Cisplatin
siCon
siAIFM2
siCon
siAIFM2
50 μm
D
Veh
Cisplatin
Veh
iFSP
Veh
iFSP
GPX4
Actin
Rel Intensity (GPX4/Actin)
1.5
1.0
0.5
0.0
**
N.S
*
Con_Veh
iFSP_Veh
Con_Cis
iFSP_Cis
E
Rel. MDA level
3
2
1
0
**
N.S
*
Con_Veh
iFSP_Veh
Con_Cis
iFSP_Cis

Supplementary Figure 5. Downregulation and inhibition of AIFM2 increases ferroptotic responses in HK2 cells. (A-C) HK2 cells were transfected with siControl or siAIFM2 as indicated, and 48 h later, the cells were treated with cisplatin (10 μM) for 24 h. (A) The protein levels of GPX4 were detected by immunoblotting. The relative protein levels are shown. The values for siControl group were set to 1 (n = 3). (B) The relative levels of MDA are shown. The values for siControl-transfected and vehicle-treated group were set to 1 (n = 4). (C) HK2 cells were transfected with siControl or siAIFM2 as indicated, and after 48 h, the cells were incubated with C11-BODIPY 581/591 (2 μM) and Hoechst 33258 for counterstaining; the images were then immediately visualized by confocal microscopy. Confocal microscopy showed non-oxidized lipid (red, Texas Red) and oxidized lipid (green, FITC). Scale bar, 50 μm. (D and E) After treatment with iFSP1 (3 μM), an inhibitor of AIFM2 (FSP1), for 2 h, HK2 cells were treated with cisplatin (10 μM) for another 24 h. (D) The protein levels of GPX4 were detected by immunoblotting. The relative protein levels are shown. The values for the vehicle group were set to 1 (n = 3). (E) The relative levels of MDA are shown. The values for siControl-transfected and vehicle-treated group were set to 1 (n = 4). All values are presented as the mean ± SD. Statistical significance was measured using one-way ANOVA with Bonferroni post hoc-test. *P<0.05, **P<0.005, N.S: Not Significant.

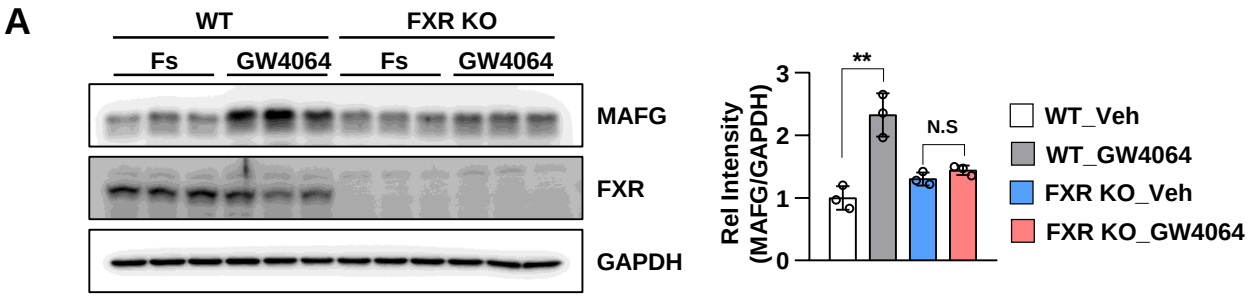

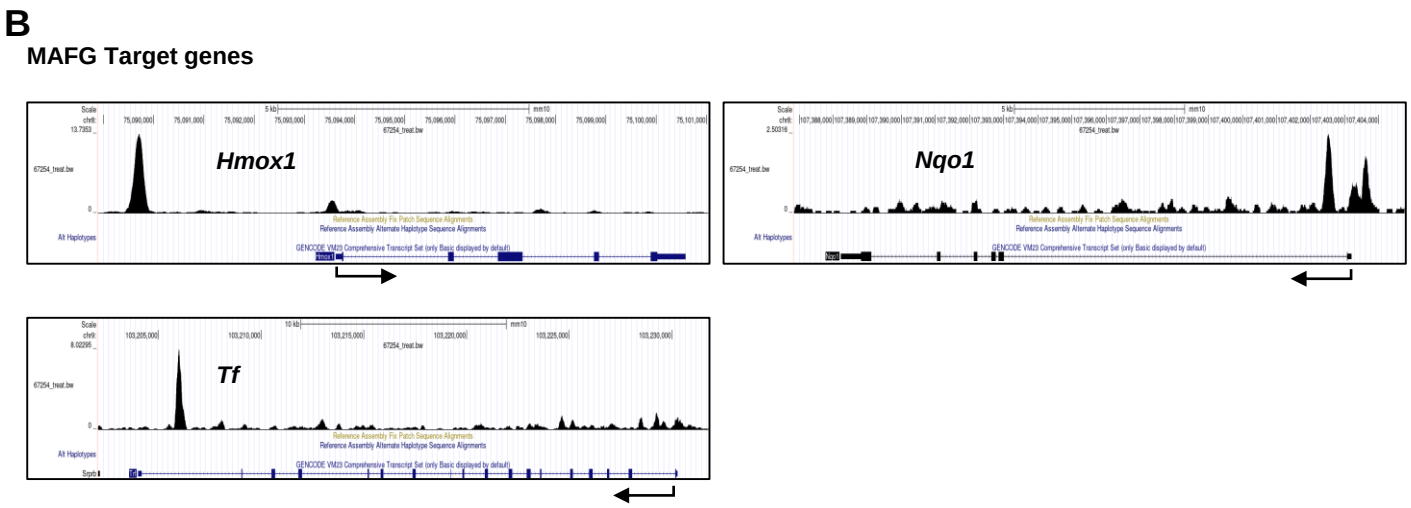

Supplementary Figure 6. FXR-dependent MAFG increases its binding to ferroptosis associated genes. (A) WT and FXR KO mice were fasted overnight (16 h) and were subsequently administered GW4064 or vehicle by oral gavage. After 4 h of GW4064 administration, the kidneys tissues were collected. Protein levels of MAFG and FXR were detected by immunoblotting. The relative protein levels are shown. The values for fasting WT mice group were set to 1 (n = 3). (B) Figures were generated from mouse liver ChIP-seq data using the University of California, Santa Cruz (UCSC) genome browser. The direction of gene transcription is indicated by the arrow and the beginning of the arrow indicates the transcription start site. All values are presented as the mean ± SD. Statistical significance was measured using one-way ANOVA with Bonferroni post hoc-test. **P<0.005, N.S: Not Significant.

Supplementary Table 1. Mouse qPCR primer sequences		
	Forward	**Reverse**
Gpx4	CCGGCTACAACGTCAAGTTT	ACGCAGCCGTTCTTATCAAT
Hmox1	CAAAGACCAGAGTCCCTCACA	GTCTGGGATGAGCTAGTGCTG
Acsl4	ACCCCAGAGGTGAGATTGTG	AATATCGCCAGTGCAAAACC
Gstp1	CCCAAGTTTGAGGATGGAGA	CCCCATCATTCACCATATCC
Gstp2	CCCAAGTTTGAGGATGGAGA	CCCCATCATTCACCATATCC
Gsta3	GGGAAGCCAGTCCTTCATTAC	TCCCATCACTTCGTAACCTTG
Ggt6	ATTTGCTTCATGCCCACTTC	TGGTATGGCAGAACAATGGA
Slc51α	GTTGCCATTTTTCTGGAGGA	GACCAAAGCAGCAGAACACA
Slc51β	ATCCTGGCAAACAGAAATCG	GGCCAAGTCTGGTTTCTCTG
Osgin1	CTTTGCCCGTCACTACAACAT	GGGCTAGGAGACAAGATGGAC
MafG	CGAGAGTTGAACCAGCACCT	TCCAGCTCCTCCTTCTGTGT
Gsta4	CCGTTACTTCCCAGTGTTTGA	CCACCATCAAAATGGCTTCTA
Aifm2	TCCGGGTAAATGCAGAACTC	CTCCAGCCAGTCTTCCACTC
Amacr	AAACAGCCTCGAGGACAAAA	CTGGGGTTCTATGGCACCTA
Dgkd	TCAACAGTATTGACTCCGATGG	TTCACACCTTGATTGTCTCCAC
Plin5	CACCTTTGCTGATGCACACT	TCCAGGAACTCATCCACACA
Tysnd1	CTGGAAGAGGAGCTGAATGG	GTGATGGGGATGCTGAAGTT
Cryab	TCTCTCCGGAGGAACTCAAA	TCCGGTACTTCCTGTGGAAC
Aldh1a3	CATCAAACCCACGGTCTTCT	TCACCTCCTCCAGGTTTTTG
Acox2	ATCTTGGCATGTTGGTGACA	CACTAGGCCGAAGACGAGAC
Lpin1	TGCAGTTTGTGAACGAGGAG	TGGAAGGGGAATCTGTCTTG
Acnat2	CTGCCTGAGAAACCACAAGAG	CTAGCCCAATCTCTGCTCCTT
Nqo1	TTCTGTGGCTTCCAGGTCTT	GGCTGCTTGGAGCAAAATAG
Cyp4a14	TATGTCCTCTGATGGACGTTTG	ATTCTGGCAAACAAGAGGATGT
Acox1	TTGGAAACCACTGCCACATA	AGGCATGTAACCCGTAGCAC
Plin2	GGAGTGGAAGAGAAGCATCG	TGGCATGTAGTCTGGAGCTG
Fabp1	CCAGAAAGGGAAGGACATCA	GTCTCCAGTTCGCACTCCTC
Acsl1	CCGGATGTTCGACAGAATTT	ATCCCACAGGCTGTTGTTTC
Ehhadh	TGGATGTGGATGACATTGCT	GGGGAAGAGTATCGGCTAGG
Cyp4a12a	GCCTTCATCACAACCCAACT	TCAGCTCATTCATCGCAAAC
Cyp4a12b	GCCTTCATCACAACCCAACT	TCAGCTCATTCATCGCAAAC
Apoa4	ATGCCAAGGAGGCTGTAGAA	CCCACTCAGCTGTACGACAA
Igf1	GGCATTGTGGATGAGTGTTG	GTCTTGGGCATGTCAGTGTG
Igfbp5	TGCACCTGAGATGAGACAGG	GAATCCTTTGCGGTCACAGT

Supplementary Table 2. Mouse ChIP-qPCR primer sequences		
	Forward	**Reverse**
Slc51α	CCCAGCTACCTCATTCCTGA	AAAGTCCAGGGCTGTGAGTG
Slc51β	CTCTGCCCTTAGCACACACC	GAGACAGAGAACCGGAGTGG
Osgin1	TCAAACTGAACCCGGGAAG	CCAAGGCTAGCAGGGGTATT
Mafg	CGACACAGGGTGTTTCACAA	TCCCAGCCTAGGTACACAAGA
Aifm2	TAGTCCTTGCCACCTGAACC	CACTAGGGGGAAGCACTCAC
Ggt6	GTCTCTGACTCCGCCTTCTG	AGCCTAGGTGTGGCTTAGCA
Gsta4	GGGAAACAAAGCGTTAACCA	ACACGCACGCACACACAT
Hmox1	AAAAGGCACAAAGAGCTCCA	TTCCGGAACCTTTTACCAAC
Nqo1	GACCAGGCTACCTTGGAACTT	GCCTGATTTCTACGGCTCTG
TF	GTCCAAAGGAAGGTGTTGGA	GATTAAAGGCGTGCTTCACC